Optomechanical Shutter Modulated Broad-Band Cavity–Enhanced Absorption Spectroscopy of Molecular Transients of Astrophysical Interest

Anton Walsh,[†] Dongfeng Zhao,[†] Wim Ubachs,[‡] and Harold Linnartz*,[†]

[†]Raymond and Beverly Sackler Laboratory for Astrophysics, Leiden Observatory, University of Leiden, P.O. Box 9513, NL 2300 RA Leiden, The Netherlands

[‡]LaserLaB, Department of Physics and Astronomy, VU University Amsterdam, De Boelelaan 1081, NL 1081 HV Amsterdam, The Netherlands

S *Supporting Information*

ABSTRACT: We describe a sensitive spectroscopic instrument capable of measuring broad-band absorption spectra through supersonically expanding planar plasma pulses. The instrument utilizes incoherent broad-band cavity-enhanced absorption spectroscopy (IBBCEAS) and incorporates an optomechanical shutter to modulate light from a continuous incoherent light source, enabling measurements of durations as low as ~400 μs. The plasma expansion is used to mimic conditions in translucent interstellar clouds. The new setup is particularly applicable to test proposed carriers of the diffuse interstellar bands, as it permits swift measurements over a broad spectral range with a resolution comparable to astronomical observations. The sensitivity is estimated to be better than 10 ppm/pass, measured with an effective exposure time of only 1 s.
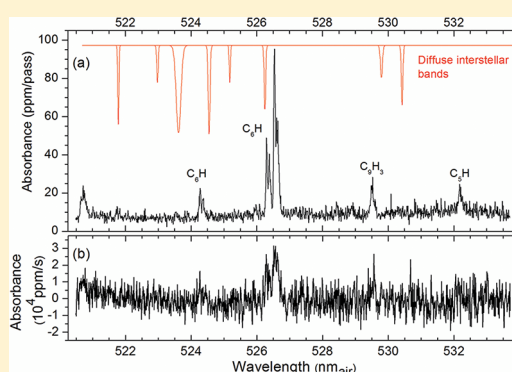
1. INTRODUCTION

The diffuse interstellar bands (DIBs) are a collection of hundreds of visible and near-infrared absorption features observed in light of stars crossing diffuse and translucent clouds. DIBs were discovered in 1921,[1] and today their origin is still as mysterious as 90 years ago.[2−6] More than 400 DIBs have been tabulated,[2,7−11] covering large spectral regions between roughly 4400 and 7000 Å and extending into the near-infrared (NIR).[12] DIB features are observed along many lines of sight, contain principally invariant central wavelengths and band widths, that can be narrow (as low as 0.1 Å) and broad (up to 20 Å). The majority of DIBs are rather weak; the weakest detected have equivalent widths less than 1 mÅ, but a number of stronger DIBs have equivalent widths over 2000 mÅ. Poor correlations between individual DIBs suggest that one single carrier is unlikely to explain all features, but they may originate from a particular family of molecules. Early hypotheses focused on grain related carriers, later this premise was discarded and now the carriers are generally believed to be molecular. Several families of potential carriers have been suggested and investigated, including complex species, PAH cations,[13,14,16,15,17] carbon chain radicals,[18−24] fullerenes,[25−29] and excited molecular hydrogen,[30,31] yet still no definite match has been made.

Testing these candidates has presented a large challenge in the laboratory, simulating the cold harsh conditions of the interstellar medium under fully controlled conditions, and a number of different techniques have been used. Spectroscopic surveys using mass selective low-temperature matrix isolation tools,[23,32−37] have been applied as a guide for where to search for unperturbed gas phase spectra. Molecular beams and jets coupled with discharge[38−42] or laser vaporization/photolysis sources[43−45] have been used to generate adiabatically cooled transients, as in the diffuse interstellar medium intense radiation fields are expected to favor formation of unstable species. A series of highly sensitive detection techniques have been subsequently applied to record accurate gas phase absorption frequencies of potential DIB carriers, e.g., resonance enhanced multiphoton ionization (REMPI),[46,47] electron photodetachment,[42,48,49] and degenerate four-wave mixing (4WM) spectroscopy,[50,51] as well as frequency plasma double modulation[52,53] and pulsed/continuous-wave cavity ring-down (CRD) spectroscopy.[39,40,54−56] In the recent past, this has led to a few tentative assignments of DIBs, specifically C_7^-,[57] l-$C_3H_2^-$,[58] C_3H_2,[59] and HC_4H^+,[60] but follow-up experimental and observational studies[22,61−63] showed that the proposed assignments are incorrect. In addition, a full coincidence was found between a broad DIB around 5450 Å and a feature measured in a hydrocarbon plasma.[64] The feature is likely
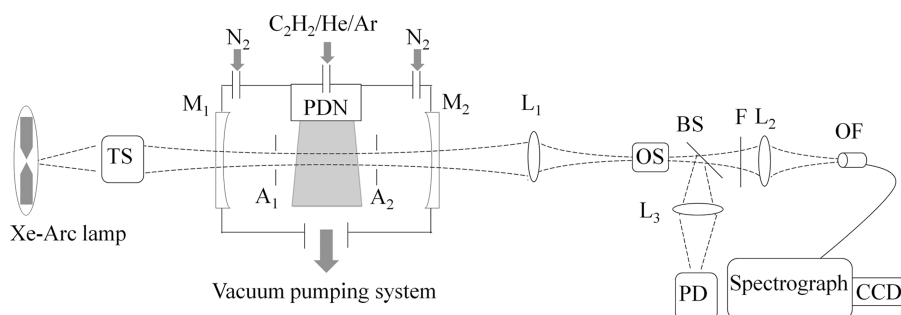
Figure 1. Experimental setup. Legend; TS, telescope; M_1 and M_2, high reflectivity mirrors; PDN, pulsed discharge nozzle; A_1 and A_2, apertures; L_1 and L_2, achromatic lenses (focal length: 7.5 cm); OS, optomechanical shutter; BS, beam splitter (10:1); L_3, lens (focal length 5 cm); PD, photodiode; F, interference filter; OF, circular to rectangular optic fiber bundle; CCD, charge coupled device. N_2 gas is admitted into the chamber near the mirrors, providing gas curtains that prohibit contaminations on the mirrors.

lifetime broadened but could not be assigned to a specific molecule.

In the present work, we introduce a new experimental concept, presenting a sensitive instrument capable of swiftly recording gas phase absorption spectra of transients created in a slit pulsed discharge nozzle, with spectral resolution equivalent to astronomical observations. This facilitates proficient testing of potential candidates of DIB carriers. The performance of the technique is demonstrated on the basis of electronic transitions of a series of hydrocarbon species.

High-pressure pulsed planar plasma expansions, have proved to be very successful in producing large abundances of highly reactive molecular transients, such as carbon chain radicals[65,66] and polycyclic aromatic hydrocarbon cations (PAHs).[40,41,67] Slit pulsed discharge nozzles offer an extension to discharge cells, largely pioneered by Oka et al.,[68,69] as low rotational temperatures (∼15 K) can be realized in a generally Doppler free environment. In a pulsed discharge nozzle, a high voltage (HV) discharge is placed across a high-pressure supersonic pulsed expansion. Combined with different absorption detection techniques, frequently CRD spectroscopy,[70,71] supersonically expanding plasma has been widely used to search for spectra of astrophysically relevant species. In a conventional CRD scheme, light from a pulsed laser is incident on an optically stable cavity, containing the sample under investigation, constructed by two high reflectivity (HR, typically $R >$ 0.9999) plano-concave mirrors. A small portion of light enters the cavity and is trapped between the two HR mirrors. Subsequently, the absorbance of the sample can be retrieved by fitting a monoexponential decay to the time dependent intensity of light leaking out of the cavity, referred to as the "ring-down" time. The main advantage of the CRD technique is the high effective path length of the light trapped inside the cavity (making 10^4–10^5 trips through the sample), resulting in an absorbance sensitivity better than 10^{-6} per pass.[72] Furthermore, CRD is insensitive to laser power fluctuations as not the absolute absorption is measured but instead a decay rate is determined.

A practical drawback of conventional CRD is that only a single wavelength absorption can be measured from a single ring-down event. A stepwise approach is necessary to record a spectrum, scanning the laser's wavelength across the absorption features of the sample. This approach is generally very time-consuming when covering large spectral ranges, particularly at high spectral resolution. Furthermore, it is difficult to measure different signals of the same carrier molecule simultaneously, which prohibits absolute intensity comparisons, e.g., in a

vibronic progression. Therefore, considering the DIBs range from 4400 Å to the near-IR, a broad-band cavity-enhanced absorption spectroscopy (BBCEAS) technique is fully complementary to the currently employed techniques, in performing a survey of spectra.

A number of broad-band cavity-enhanced approaches have been pioneered in the past 15 years,[73] including broad-band cavity ring-down,[74] frequency comb broad-band cavity ring-down spectroscopy,[75] multiplex integrated cavity output spectroscopy (MICOS),[76] Fourier transform cavity-enhanced absorption spectroscopy using a broad-band dye laser or Xe-arc lamp,[77,78] cavity-enhanced plasma self-absorption spectroscopy (CEpSAS),[79] and incoherent broad-band cavity-enhanced absorption spectroscopy (IBBCEAS).[80] In IBBCEAS, an incoherent light source, such as a Xe-arc lamp, light emitting diode (LED) or supercontinuum laser, is continuously coupled into an optical cavity, consisting of two HR mirrors. Light transmitted through the cavity is dispersed by a grating onto a diode array or charge-coupled device (CCD) array. The CCD/diode array is usually exposed to light for only a number of seconds. The absorbance is calculated from the measurement of integrated light transmitted through the optical cavity. Subsequently, a portion of a sample's absorption spectrum, often sufficient to identify multiple species, can be obtained in a single observation. The absorbance (A) is calculated using the light transmitted through an empty cavity (I_0), through the sample containing cavity (I) and reflectivity of the mirrors (R);

$$A = \left(\frac{I_0}{I} - 1 \right)(1 - R) \qquad (1)$$

The spectral resolution is limited by the wavelength selection element, grating, and the pixel size of the CCD detector/diode array and is generally lower than in CRD, where pulsed or continuous wave (cw) lasers are used with bandwidths of the order of 0.05 and 0.001 cm^{-1}, respectively. IBBCEAS, however, offers a large spectral coverage with high effective pathlengths in combination with experimental simplicity and short data accumulation times.

IBBCEAS has been applied in a number of different fields, principally in trace gas detection,[81,82] continuous supersonic jets,[83] surface adsorbed,[84,85] and liquid phase[86,87] studies. So far, the optical losses measured have not been time-gated and in the majority of cases are approximately constant for a number of seconds. Consequently, accumulation of light is relatively straightforward. However, in a pulsed discharge nozzle source the sample exists for ∼500 μs and is generally employed at less than 20 Hz, leading to an exceedingly low duty cycle (∼0.01)
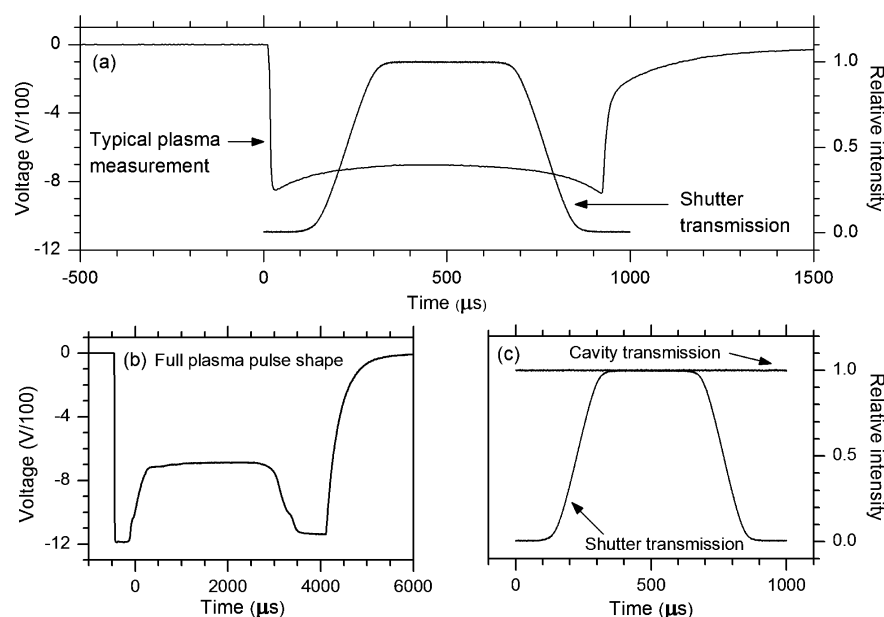
Figure 2. Light exiting the cavity is only transmitted through the shutter when the plasma strikes and is monitored using a photodiode. The signal from the photodiode and voltage at one of the jaws is made to coincide in time using a set of pulse and delay generators. Typical overlapping signals from the photodiode and plasma are shown in (a). The temporal profile of the full gas pulse, through the slit, is visualized by extending the length of the discharge pulse to several milliseconds and by monitoring the voltage at one of the jaws; see (b). Comparison of the relative intensity of light exiting the cavity with light transmitted through the shutter, measured using a photodiode is shown in (c).

for an IBBCEAS measurement. This reduces its signal-to-noise ratio (S/N) substantially, consequently also reducing sensitivity. To overcome this, we incorporate an optomechanical shutter as a time-gate, modulating the detection scheme of IBBCEAS, in which way the effective duty cycle is improved and reaches a value close to unity. Accordingly, a simple technique to proficiently test the hypothesis of different candidates as DIB carriers, over a relatively large spectral range (where high reflectivity mirrors are available) and with resolutions comparable to astronomical observations, is established.

2. INSTRUMENTATION

The instrument is described in the following three subsections: section 2.1 focuses on the production of transients in a pulsed discharge nozzle source, section 2.2 describes the observation of transients using an IBBCEAS setup, and section 2.3 illustrates the timing aspects of the instrument. A schematic of the complete setup is shown in Figure 1.

2.1. Pulsed Discharge Nozzle Source. A number of carbon chains, bare and hydrogen/nitrogen/oxygen-capped, and related ions have been identified in dense interstellar clouds and play an important role in the chemistry of the interstellar medium.[88−91] As a result, they have become likely candidates as carriers of the DIBs and are the focus of the present study. A pulsed planar discharge expansion of 0.5% C_2H_2, diluted in a 1:1 He/Ar precursor gas mixture is employed to form carbon chain transients. The production technique has been described in detail elsewhere[38,65,66] and will only be discussed briefly here, with typical settings for the measurements presented. A supersonically expanding gas pulse of ~2 ms is released into a vacuum chamber, pumped by a roots blower system of pumping capacity 3600 m^3/h, by a pulsed nozzle (General Valve, Series 9) with a 2 mm orifice. A multichannel inlet system disperses the gas pulse over a 3 cm × 400 μm slit. The backing pressure of the precursor gas behind the valve is ~12

bar. The valve is run at 4 Hz and during experiments the typical chamber pressure is approximately 1×10^{-2} mbar. The dispersed gas pulse travels through a grounded metallic plate, with a slit, and two metal jaws. The two metal jaws act as cathodes. The grounded plate and cathode jaws are separated by a ceramic spacer, also with a slit. The ground plate is separated from the nozzle body by a second slotted ceramic spacer. A negative voltage of approximately −1200 V is applied to the metal jaws for between 500 and 1000 μs, as the expanding gas pulse moves through the nozzle system and strikes toward the grounded metal plate. The gas pulse is monitored by measuring the voltage drop, and current increase, across one of the jaws of the slit (Figure 2a). The full gas pulse can also be visualized by extending the voltage discharge to several milliseconds, i.e., longer than the gas pulse (Figure 2b).

2.2. IBBCEAS Setup. The pulsed discharge nozzle is aligned with its slit along and approximately 7 mm above the optical axis of a high finesse cavity. The optical cavity comprises two identical HR mirrors, ~0.999 95 reflectivity between 520 and 560 nm. Light from a 300 W Xe-arc lamp is coupled into the optical cavity using a small telescope. A set of apertures placed inside the cavity are used to block that part of the light beam that does not cross the plasma expansion, or light scattered from the chamber walls. In this configuration, the plasma is probed between 4 and 10 mm below the slit. Light leaking out of the cavity is focused onto the entrance of a homemade optomechanical shutter, described in section 2.3, which modulates the light to ~500 μs pulses. After modulation, the broad-band light is spectrally narrowed by an interference bandpass filter to the spectral range of the HR mirrors and is focused onto a circular to rectangular optic fiber bundle (each fiber has a diameter of 50 μm). Light exiting the optical fiber is incident on a 13 μm slit entrance of a spectrograph (Shamrock 750 equipped with a 750 mm focal length and a 1800 lines/mm grating). The spectrograph disperses light onto a charge-coupled device (Andor Newton CCD containing 2048 × 528

pixels of 13.5 μm width). Each individual spectral recording covers a 200 Å wavelength range, with a spectral resolution of 0.3 Å. A higher resolution is also possible using a higher order grating. However, this limits the wavelength range that can be measured in a single observation. A compromise between resolution and wavelength range is made. Therefore, a resolution of 0.3 Å is selected to facilitate the measurement of laboratory spectral features that can possibly coincide with both narrow (~1 Å) and broad (~20 Å) DIB bandwidths, while keeping a relatively large wavelength range (~200 Å). The absolute wavelength accuracy is 0.1 Å per pixel, proficient for measuring spectral features of bandwidths comparable to the DIBs.

2.3. Experiment Timing. A homemade optomechanical shutter constructed from a voice-coil actuator[92,93] is applied to modulate light exiting the cavity. The shutter has an opening rise time of ~17 μs for focused coherent light from a He−Ne laser. For focused incoherent light exiting the cavity the rise time is ~100 μs. This increase in rise time of light exiting the cavity is due to the extended focus of the Xe-arc lamp.[94] The shutter transmits light only when the plasma is present in the cavity. To monitor the opening/closing of the shutter, a beam splitter directs a portion (10%) of the light transmitted through the cavity onto a photodiode. Figure 2c compares the intensity of light transmitted through the cavity, measured directly at the exit of the cavity using the same photodiode, against light transmitted through the shutter, placing the photodiode after the shutter. The width of the discharge pulse is chosen to be slightly longer than the opening time of the shutter. The plasma and shutter are set coincidental using a set of pulse generators and delays. A sample signal of the overlapping voltage drop across one of the jaws of the discharge and the intensity of light transmitted through the shutter is shown in Figure 2a. The improvement in sensitivity, due to an increase of S/N, from the employment of an optomechanical shutter will be discussed in the following section.

The optomechanical shutter is placed after the cavity to modulate not only light from the Xe-arc lamp but also light emitted from the plasma itself. This is necessary as the plasma length is longer than the shutter opening time. For measurement of I, both the Xe-arc lamp and light emitted from the plasma is modulated. For measurement of BG_{plasma}, the light emitted from the plasma is modulated alone. This enables direct comparison between I and BG_{plasma}.

3. RESULTS AND DISCUSSION

The CCD is exposed to light for 90 s at a time, and data are accumulated for 15 min. This results in an effective exposure time of only ~1 s, for a plasma duration of 500 μs. Two background measurements are made: a background dark current, where the light source is blocked and the plasma is not running (BG), and a background measurement while the plasma is running and the light source is blocked (BG_{plasma}). BG_{plasma} is subtracted from I, to remove the effects of light emission from the plasma. Reflectivity (R) of the cavity mirrors in the present experiment are measured using CRD in advance (see the Supporting Information). The absorbance (A) is calculated using the equation

$$A = \left(\left(\frac{I_0 - BG}{I - BG_{plasma}}\right) - 1\right)(1 - R) \qquad (2)$$
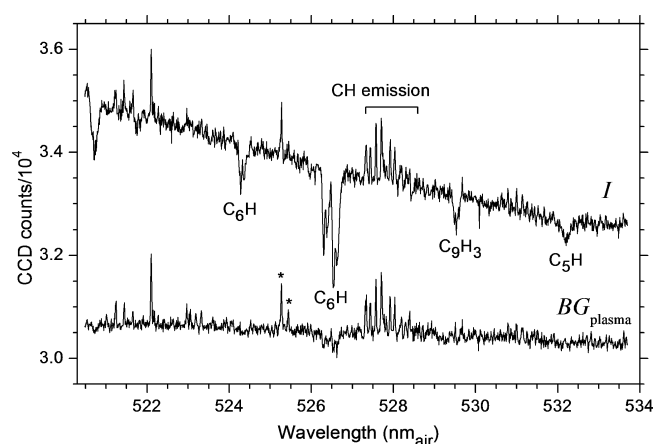
Figure 3. I: transmission through the cavity while the lamp and plasma are running. BG_{plasma}: transmission through the cavity while only the plasma is running. Argon emission lines are marked with asterisks and are used for additional wavelength calibration. Units of spectra are in absolute counts. The effective exposure time is only ~1 s for both spectra; absorption and emission spectra can be observed with exposure times of a few seconds.

A sample measurement of I and BG_{plasma} is shown in Figure 3, between 520.5 and 534 nm. All values are given in nanometers in air. Absorption features (sharp decreases in transmission) and emission features (sharp increases in transmission) can both be seen in the transmission spectrum I. Emission of CH and argon are clearly visible. Absorption features of C_6H (~524.5, 526.5, and 526.7 nm), C_9H_3 (~529.6 nm), and C_5H (~532.4 nm) are visible.[39,66,95−97] An unidentified band is located at 520.9 nm. The same emission features seen in I are observed in BG_{plasma}. Weak absorption features can also be found, e.g., at ~526.7 nm. These weak features are due to self-absorption of light emitted by the plasma, enhanced by the optical cavity. The underlying process, cavity-enhanced plasma self-absorption spectroscopy (CEp-SAS), has been described in detail in ref 79. The plasma background removed transmission of light through the cavity while the plasma is running, $I-BG_{plasma}$, is shown in Figure 4. The transmission curve is devoid of any emission features. The dark current removed transmission through the vacant chamber, I_0-BG, is shown as well. The spectrum is featureless, and is smoothened for analysis.

The processed absorbance spectrum is shown in Figure 5a. Using calculated oscillator strengths,[98] the C_6H expansion densities are estimated to be ~$10^{10}-10^{11}$ molecules/cm^3. The maximum absorbance of the C_6H R-branch peak of the $B^2\Pi_{3/2}-X^2\Pi_{3/2}$ spin−orbit component is estimated from previous CRDS measurements to be 150 ± 20 ppm per pass, in agreement with the absorbance measured here. Figure 5a compares the laboratory spectrum of the expanding hydrocarbon plasma with simulated DIBs. The DIB spectrum is calculated from a catalog of diffuse interstellar bands reported from echelle spectra of the double-lined spectroscopic binary HD 204827.[10] There are no convincing coincidences between spectra recorded through the hydrocarbon plasma and the listed DIBs. However, it is clear that the spectra measured with the current setup, in a very short time, are directly comparable to DIB spectra, without the necessity of further calculations, such as convolution or molecular modeling. Equivalent widths of different DIBs can also be directly compared, which is an
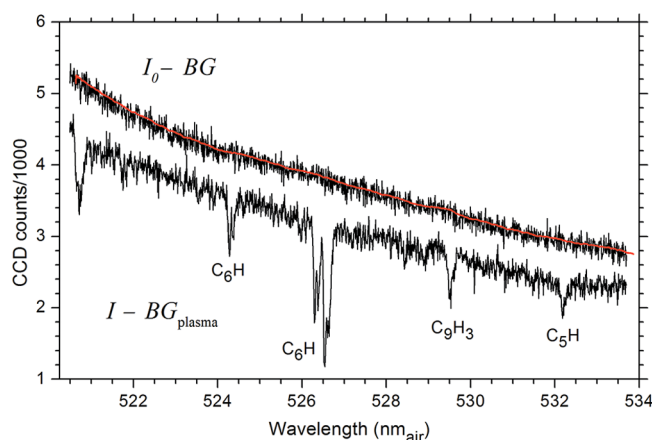
Figure 4. $I_0 - BG$: dark current subtracted measurement of transmission through the cavity while only the lamp is running. A smoothed plot, used for analysis, is shown in red. $I - BG_{plasma}$: light from the lamp source transmitted through the cavity while the plasma is running. The effects of light created by the plasma in the chamber are removed. Solely absorption features, sharp decreases in the transmission, remain. Units of spectra are in absolute counts.
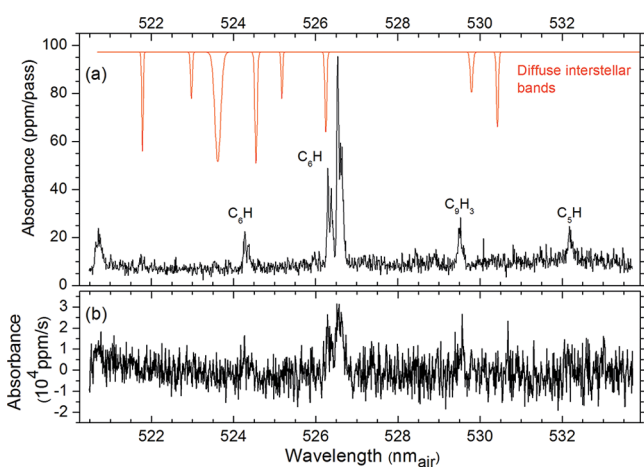
Figure 5. (a) Processed spectrum of hydrocarbon plasma (black), in units of ppm per pass. Diffuse interstellar bands (red) observed in the spectrum of HD 204827[10] are also shown. (b) Spectrum measured without modulation, demonstrating the significant improvement in S/N that is obtained by using optomechanical shutter modulation. The pulsed discharge nozzle is run at a higher repetition rate of 20 Hz. Other plasma parameters are the same as the measurement shown in (a). As the optical losses inside the cavity are time-dependent, units of average absorbance per second are used.

important criterion in accessing DIBs through adjacent vibronic bands.

Optomechanical shutter modulation is a necessity for the observation of weak transient absorption in the plasma. Fast-time-gating, $\sim$500 μs, of a linear array of pixels for each plasma event results in a poor S/N ratio of 2:1 in I_0. The majority of charge collected from pixels is due to dark current of the detector, which is measured separately and subtracted from the transmission signal. Because dark current depends on the detector, accumulation of light from several exposures does not decrease noise, due to dark current.[80] Consequently, accumulating, using fast-time-gating, for periods up to several hours does not improve S/N effectively, even though the duty cycle is close to one. In fact, higher sensitivity can be achieved

using a lower duty cycle, running the discharge nozzle at higher repetition rates and using longer exposure times. A spectrum measured using this technique is shown in Figure 5b. For this measurement the pulsed discharge is run at 20 Hz and no modulation is used. The CCD is exposed to light for 3 s at a time, and data are accumulated for 15 min. The CCD exposure time is reduced because without modulation the detector will become saturated for exposure times longer than 3 s. Other settings remain the same. The strong C_6H feature, however, is only just visible. Modulation improves the S/N level to better than 15:1 in I_0, resulting in a significant enhancement in sensitivity.

In theory the pulsed setup can have the same sensitivity as a standard, i.e., nonpulsed, IBBCEAS setup. Fluctuations in the lamp intensity are not crucial, as mainly a spectral identification is required and not necessarily accurate absolute absorbance measurements. The limited plasma duration of <1 ms necessitates longer measurement times. For the spectra shown in Figure 5a, the plasma duration is $\sim$500 μs and the transmission of the cavity is measured for 15 min. This gives a total exposure time of only $\sim$1 s to the plasma products. The sensitivity can be further improved by using longer exposure times, increasing the S/N level. However, this diminishes the specific advantage of IBBCEAS compared with regular CRD, where slow scanning is an intrinsic property. Comparing the current IBBCEAS measurement, shown in Figure 5a, with CRD measurements using the same plasma source gives a sensitivity estimated at 10 ppm. Actually, the sensitivity is higher, as the CRD measurement is made at the densest area of the plasma. The IBBCEAS absorbance measurement is an average of the optical losses over a 6 mm cross-section. The density of C_6H at the periphery is lower, and so the absolute absorbance measured is less than 150 ppm. This is both an advantage and disadvantage of the current the setup. A large cross-section of the plasma is probed, but it is difficult to study the plasma spatially. If a particular transient, with weak oscillator strength, has substantially higher abundances in specific regions (i.e., 10 mm downstream from the nozzle orifice), a CRD technique, with superior spatial resolution, may be more suitable, but otherwise IBBCEAS offers a much more convenient way to search for spectral features.

4. CONCLUSION

In conclusion, we have presented a new technique for measuring absorption of pulsed plasma events over a relatively large wavelength range, using a pulsed discharge nozzle. The main advantage of the setup is its low time consumption, needing very little data analysis. This makes the setup flexible and allows dealing with chemically different samples, probed under different conditions in rather short time periods. The setup presented here shows potential to test the hypothesis of carbon chain radicals as carriers of the DIBs, but the setup is easily adaptable to test other potential carriers, such as PAH cations. If necessary, portions of the spectrum can be complimented with further investigation by regular high resolution CRD.[66] As the Xe-arc light source has a large spectral coverage, the setup also offers the prospect of examining carrier candidates up to the near-IR, a region where dye lasers, for example, are harder to operate.

The concept presented here is principally different from all previous techniques used to search for potential DIB carriers, and its potential lies particularly in its applicability. The latter obviously reaches far beyond the field of DIB research and the

technique described here also will have use as a general plasma diagnostics tool.

■ ASSOCIATED CONTENT

ⓢ Supporting Information

Reflectivity curve for cavity mirrors, measured using CRDS. This material is available free of charge via the Internet at http://pubs.acs.org.

■ AUTHOR INFORMATION

Corresponding Author

*E-mail: linnartz@strw.leidenuniv.nl.

Notes

The authors declare no competing financial interest.

■ ACKNOWLEDGMENTS

■ REFERENCES

(1) Heger, M. L. *Lick Obs. Bull.* **1922**, *337*, 141−145.
(2) Herbig, G. H. *Annu. Rev. Astrophys.* **1995**, *33*, 19−73.
(3) *The Diffuse Interstellar Bands*; Tielens, A. G. G. M., Snow, T. P., Eds.; Kluwer Academic: Dordrecht, Netherlands, 1995.
(4) Snow, T. P. *Spectrochim. Acta Part A* **2001**, *57*, 615−626.
(5) Krelowski, J. *Adv. Space Res.* **2002**, *30*, 1395−1407.
(6) Sarre, P. J. *J. Mol. Spectrosc.* **2006**, *238*, 1−10.
(7) Jenniskens, P.; Desert, F.-X. *Astron. Astrophys. Suppl. Ser.* **1994**, *106*, 39−78.
(8) Galazutdinov, G. A.; Musaev, F. A.; Krelowski, J.; Walker, G. A. H. *PASP* **2000**, *112*, 648−690.
(9) Tuairisg, S. O.; Cami, J.; Foing, B. H.; Sonnentrucker, P.; Ehrenfreund, P. *Astron. Astrophys. Suppl. Ser.* **2000**, *142*, 225−238.
(10) Hobbs, L. M.; York, D. G.; Snow, T. P.; Oka, T.; Thorburn, J. A.; Bishof, M.; Friedman, S. D.; McCall, B. J.; Rachford, B.; Sonnentrucker, P.; et al. *Astrophys. J.* **2008**, *680*, 1256.
(11) Cordiner, M. A.; Cox, N. L. J.; Evans, C. J.; Trundle, C.; Smith, K. T.; Sarre, P. J.; Gordon, K. D. *Astrophys. J.* **2011**, *726*, 39.
(12) Geballe, T. R.; Najarro, F.; Figer, D. F.; Schlegelmilch, B. W.; de la Fluente, D. *Nature* **2011**, *728*, 200−202.
(13) Crawford, M. K.; Tielens, A. G. G. M.; Allamandola, L. J. *Astrophys. J. Lett.* **1985**, *293*, L45−L48.
(14) van der Zwet, G. P.; Allamandola, L. J. *Astron. Astrophys.* **1985**, *146*, 76−80.
(15) Halasinski, T. M.; Salama, F.; Allamandola, L. J. *Astrophys. J.* **2005**, *628*, 555−566.
(16) Brechignac, P.; Pino, T.; Boudin, N. *Spectrochim. Acta Part A* **2001**, *57*, 745−756.
(17) Salama, F.; Galazutdinov, G. A.; Krełowski, J.; Biennier, L.; Beletsky, Y.; Song, In-Ok. *Astrophys. J.* **2011**, *728*, 154.
(18) Dougloas, A. E. *Nature* **1977**, *269*, 130−132.
(19) Fulara, J.; Lessen, D.; Freivogel, P.; Maier, J. P. *Nature* **1993**, *366*, 439−441.
(20) Thaddeus, P.; McCarthy, M. C.; Travers, M. J.; Gottlieb, C. A.; Chen, W. *Faraday Discuss.* **1998**, *109*, 121−135.
(21) Motylewski, T.; Linnartz, H.; Vaizert, O.; Maier, J. P.; Galazutdinov, G. A.; Musaev, F. A.; Krełowski, J.; Walker, G. A. H.; Bohlender, D. A. *Astrophys. J.* **2000**, *531*, 312−320.
(22) McCall, B.; Thorburn, J.; Hobbs, L. M.; Oka, T.; York, D. G. *Astrophys. J. Lett.* **2001**, *559*, L49−L53.
(23) Nagarajan, R.; Maier, J. P. *Int. Rev. Phys. Chem.* **2010**, *29*, 521−554.
(24) Oka, T.; McCall, B. *Science* **2011**, *331*, 293−294.
(25) Kroto, H. W.; Jura, M. *Astron. Astrophys.* **1992**, *263*, 275−280.
(26) Foing, B. H.; Ehrenfreund, P. *Nature* **1994**, *369*, 296−298.
(27) Foing, B. H.; Ehrenfreund, P. *Astron. Astrophys.* **1997**, *319*, L59−L62.
(28) Herbig, G. H. *Astrophys. J.* **2000**, *542*, 334−343.
(29) Zhou, Z.; Sfeir, M. Y.; Zhang, L.; Hybertsen, M. S.; Steigerwald, M.; Brus, L. *Astrophys. J.* **2006**, *638*, L105−L108.
(30) Sorokin, P. P.; Glownia, J. H. *Astrophys. J.* **1996**, *473*, 900−920.
(31) Sorokin, P. P.; Glownia, J. H.; Ubachs, W. *Faraday Discuss.* **1998**, *109*, 137−163.
(32) Kratschmer, W.; Sorg, N.; Huffman, D. R. *Surf. Sci.* **1985**, *156*, 814−821.
(33) Salama, F.; Allamandola, L. J. *J. Chem. Phys.* **1991**, *94*, 6964−6977.
(34) Freivogel, P.; Fulara, J.; Lessen, D.; Forney, D.; Maier, J. P. *Chem. Phys.* **1994**, *189*, 335−341.
(35) Salama, F.; Joblin, C.; Allamandola, L. J. *J. Chem. Phys.* **1994**, *101*, 10252−10262.
(36) Bondybey, V. E.; Smith, A. M.; Agreiter, J. *Chem. Rev.* **1995**, *96*, 2113−2134.
(37) Jochnowitz, E. B.; Maier, J. P. *Mol. Phys.* **2008**, *59*, 544.
(38) Motylewski, T.; Linnartz, H. *Rev. Sci. Instrum.* **1999**, *70*, 1305−1312.
(39) Linnartz, H.; Motylewski, T.; Vaizert, O.; Maier, J. P.; Apponi, A. J.; McCarthy, M. C.; Gottlieb, C. A.; Thaddeus, P. *J. Mol. Spectrosc.* **1999**, *197*, 1−11.
(40) Biennier, L.; Salama, F.; Allamandola, L. J.; Scherer, J. J. *J. Chem. Phys.* **2003**, *118*, 7863−7872.
(41) Romanini, D.; Biennier, L.; Salama, F.; Kachnov, A.; Allamandola, L. J.; Stoeckel, F. *Chem. Phys. Lett.* **1999**, *303*, 165−170.
(42) Zhao, Y. X.; de Beer, E.; Xu, C.; Taylor, T.; Neumark, D. M. *J. Chem. Phys.* **1996**, *105*, 4905−4919.
(43) Curl, R.; Murray, K.; Petri, M.; Richnow, M.; Tittel, F. *Chem. Phys. Lett.* **1989**, *161*, 98−102.
(44) Giesen, T.; van Orden, A.; Hwang, H.; Fellers, R.; Provencal, R.; Saykally, R. *Science* **1994**, *265*, 756−759.
(45) Sumiyoshi, Y.; Imajo, T.; Tanaka, K.; Tanaka, T. *Chem. Phys. Lett.* **1994**, *231*, 569−573.
(46) Maier, J. P.; Boguslavskiy, A.; Ding, H.; Walker, G.; Bohlender, D. *Astrophys. J.* **2006**, *640*, 369−372.
(47) Boguslavskiy, A.; Maier, J. P. *J. Chem. Phys.* **2006**, *125*, 094308.
(48) Xu, C. S.; Burton, G. R.; Taylor, T. R.; Neumark, D. M. *J. Chem. Phys.* **1997**, *107*, 3428−3436.
(49) Pino, T.; Tulej, M.; Guthe, F.; Pachkov, M.; Maier, J. P. *J. Chem. Phys.* **2002**, *116*, 6126−6131.
(50) Butenhoff, T.; Rohlfing, E. *J. Chem. Phys.* **1992**, *97*, 1595−1598.
(51) Raghunandan, R.; Mazzotti, F.; Chauhan, R.; Tulej, M.; Maier, J. P. *J. Phys. Chem. A* **2009**, *113*, 13402−13406.
(52) Pfluger, D.; Sinclair, W. E.; Linnartz, H.; Maier, J. P. *Chem. Phys. Lett.* **1999**, *313*, 171−178.
(53) Sinclair, W. E.; Pfluger, D.; Linnartz, H.; Maier, J. P. *J. Chem. Phys.* **1999**, *110*, 296−303.
(54) Ball, C. D.; McCarthy, M. C.; Thaddeus, P. *J. Chem. Phys.* **2000**, *112*, 10149−10155.
(55) Birza, P.; Motylewski, T.; Khoroshev, D.; Chirokolava, A.; Linnartz, H.; Maier, J. P. *Chem. Phys.* **2002**, *283*, 119−124.
(56) Romanini, D.; Kachanov, A. A.; Sadeghi, N.; Stoeckel, F. *Chem. Phys. Lett.* **1997**, *264*, 316−322.
(57) Tulej, M.; Kirkwood, D. A.; Pachkov, M.; Maier, J. P. *Astrophys. J.* **1998**, *506*, L69−L73.
(58) Guthe, F.; Tulej, M.; Pachkov, M.; Maier, J. P. *Astrophys. J.* **2001**, *555*, 466−471.
(59) Maier, J. P.; Walker, G. A. H.; Bohlender, D. A.; Mazzotti, F. J.; Raghunandan, R.; Fulara, J.; Garkusha, I.; Nagy, A. *Astrophys. J.* **2011**, *726*, 41.
(60) Krelowski, J.; Beletsky, Y.; Galazutdinov, G. A.; Kolos, R.; Gronowski, M.; LoCurto, G. *Astrophys. J. Lett.* **2010**, *714*, L64−L67.

(61) McCall, B.; Oka, T.; Thorburn, J.; Hobbs, L. M.; York, D. G. *Astrophys. J. Lett.* **2002**, *567*, L145−L148.

(62) Krelowski, J.; Galazutdinov, G. A.; Kolos, R. *Astrophys. J.* **2011**, *735*, 124.

(63) Maier, J. P.; Chakrabarty, S.; Mazzotti, F. J.; Rice, C. A.; Dietsche, R.; Walker, G. A. H.; Bohlender, D. A. *Astrophys. J. Lett.* **2011**, *729*, L20.

(64) Linnartz, H.; Wehres, N.; van Winckel, H.; Walker, G. A. H.; Bohlender, D. A.; Tielens, A. G. G. M. *Astron. Astrophys.* **2010**, *511*, L3.

(65) Linnartz, H. Cavity Ring-Down Spectroscopy of Molecular Transients of Astrophysical Interest. In *Cavity Ring-down Spectroscopy − Techniques and Applications*; Berden, G., Engeln, R., Eds.; Wiley-Blackwell: Chichester, United Kingdom, 2009; pp 145−179.

(66) Zhao, D.; Haddad, M. A.; Linnartz, H.; Ubachs, W. *J. Chem. Phys.* **2011**, *135*, 044307.

(67) Ricketts, C.; Contreras, C.; Walker, R.; Salama, F. *Int. J. Mass Spectrom. Ion Processes* **2011**, *300*, 26−30.

(68) Oka, T. *Phys. Rev. Lett.* **1980**, *45*, 531−534.

(69) Pan, F.; Oka, T. *Phys. Rev. A* **1987**, *36*, 2297−2310.

(70) *Cavity-ringdown Spectroscopy: An Ultratrace-Absorption Measurement Technique*; Busch, K. W., Busch, M. A., Eds.; ACS Symposium Series 720; American Chemical Society: Washington, DC, United States, 1999.

(71) *Cavity Ring-down Spectroscopy − Techniques and Applications*; Berden, G., Engeln, R., Eds.; Wiley-Blackwell: Chichester, United Kingdom, 2009.

(72) O'Keefe, A.; Deacon, D. A. G. *Rev. Sci. Instrum.* **1988**, *59*, 2544−2551.

(73) Ball, S.; Jones, R. Broadband Cavity Ring-Down Spectroscopy. In *Cavity Ring-down Spectroscopy − Techniques and Applications*; Berden, G., Engeln, R., Eds.; Wiley-Blackwell: Chichester, United Kingdom, 2009; pp 57−88.

(74) Ball, S. M.; Povey, I. M.; Norton, E. G.; Jones, R. *Chem. Phys. Lett.* **2001**, *342*, 113−120.

(75) Thorpe, M. J.; Moll, K. D.; Jones, R. J.; Safdi, B.; Ye, Jun. *Science* **2006**, *311*, 1595−1599.

(76) Biennier, L.; Salama, F.; Gupta, M.; O'Keefe, A. *Chem. Phys. Lett.* **2004**, *387*, 287−294.

(77) Engeln, R.; Meijer, G. *Rev. Sci. Instrum.* **1996**, *67*, 2708−2713.

(78) Ruth, A. A.; Orphal, J.; Fiedler, S. E. *Appl. Opt.* **2007**, *46*, 3611−3616.

(79) Walsh, A. J.; Zhao, D.; Linnartz, H. *Appl. Phys. Lett.* **2012**, *101*, 09111.

(80) Fiedler, S. E.; Hese, A.; Ruth, A. A. *Chem. Phys. Lett.* **2003**, *371*, 284−294.

(81) Gherman, T.; Venables, D. S.; Vaughan, S.; Orphal, J.; Ruth, A. A. *Environ. Sci. Technol.* **2008**, *42*, 890−895.

(82) Dixneuf, S.; Ruth, A. A.; Vaughan, S.; Varma, R. M.; Orphal. *Atmos. Chem. Phys.* **2009**, *9*, 823−829.

(83) Fiedler, S. E.; Hoheisel, G.; Ruth, A. A.; Hese, A. *Chem. Phys. Lett.* **2003**, *382*, 447−453.

(84) Ruth, A. A.; Lynch, K. T. *Phys. Chem. Chem. Phys.* **2008**, *10*, 7098−7108.

(85) van der Sneppen, L.; Hancock, G.; Kaminski, C.; Laurila, T.; Mackenzie, S. R.; Neil, S. R. T.; Peverall, R.; Ritchie, G. A. D.; Schnippering, M.; Unwin, P. R. *Analyst* **2010**, *135*, 133−139.

(86) Fiedler, S. E.; Hese, A.; Ruth, A. A. *Rev. Sci. Instrum.* **2005**, *76*, 023107.

(87) Kiwanuka, S. S.; Laurila, T.; Kaminski, C. F. *Anal. Chem.* **2010**, *82*, 7498−7501.

(88) McCarthy, M. C.; Thaddeus, P. *Chem. Soc. Rev.* **2001**, *30*, 175−185.

(89) Bell, M. B.; Feldman, P. A.; Travers, M. J.; McCarthy, M. C.; Gottlieb, C. A.; Thaddeus, P. *Astrophys. J. Lett.* **1997**, *483*, L61−L64.

(90) Gottlieb, C. A.; Apponi, A. J.; McCarthy, M. C.; Thaddeus, P.; Linnartz, H. *J. Chem. Phys.* **2000**, *113*, 1910−1915.

(91) Wakelam, V.; Smith, I. W. M.; Herbst, E.; Troe, J.; Geppert, W.; Linnartz, H.; Öberg, K.; Rouo, E.; Agundez, M.; Pernot, P.; et al. *Space Sci. Rev.* **2010**, *156*, 13−72.

(92) Maguire, L. P.; Szilagyi, S.; Scholten, R. E. *Rev. Sci. Instrum.* **2004**, *75*, 3077−3079.

(93) Scholten, R. E. *Rev. Sci. Instrum.* **2007**, *78*, 026101.

(94) Fiedler, S. E.; Heitmann, U.; Hese, A. *Rev. Sci. Instrum.* **2007**, *78*, 073104.

(95) Zhao, D.; Wehres, M. N.; Linnartz, H.; Ubachs, W. *Chem. Phys. Lett.* **2011**, *134*, 232−237.

(96) Zhao, D.; Haddad, M. A.; Linnartz, H.; Ubachs, W. *J. Chem. Phys.* **2011**, *135*, 044201.

(97) Haddad, M. A.; Zhao, D.; Linnartz, H.; Ubachs, W. *Chinese J. Chem. Phys.* **2012**, *25*, 129−134.

(98) Cao, Z.; Peyerimhoff, S. D. *Phys. Chem. Chem. Phys.* **2001**, *3*, 1403−1406.

■ NOTE ADDED AFTER ASAP PUBLICATION

This article was published ASAP on January 9, 2013, with an error in eq 2. The corrected version was reposted on March 13, 2013.